Supplement of Atmos. Chem. Phys., 23, 5851–5866, 2023
https://doi.org/10.5194/acp-23-5851-2023-supplement

Supplement of

On the importance of multiphase photolysis of organic nitrates on their global atmospheric removal

Juan Miguel González-Sánchez et al.

Correspondence to: Juan Miguel González-Sánchez (juangonzalez.sc@proton.me) and Anne Monod (anne.monod@univ-amu.fr)

Table of contents

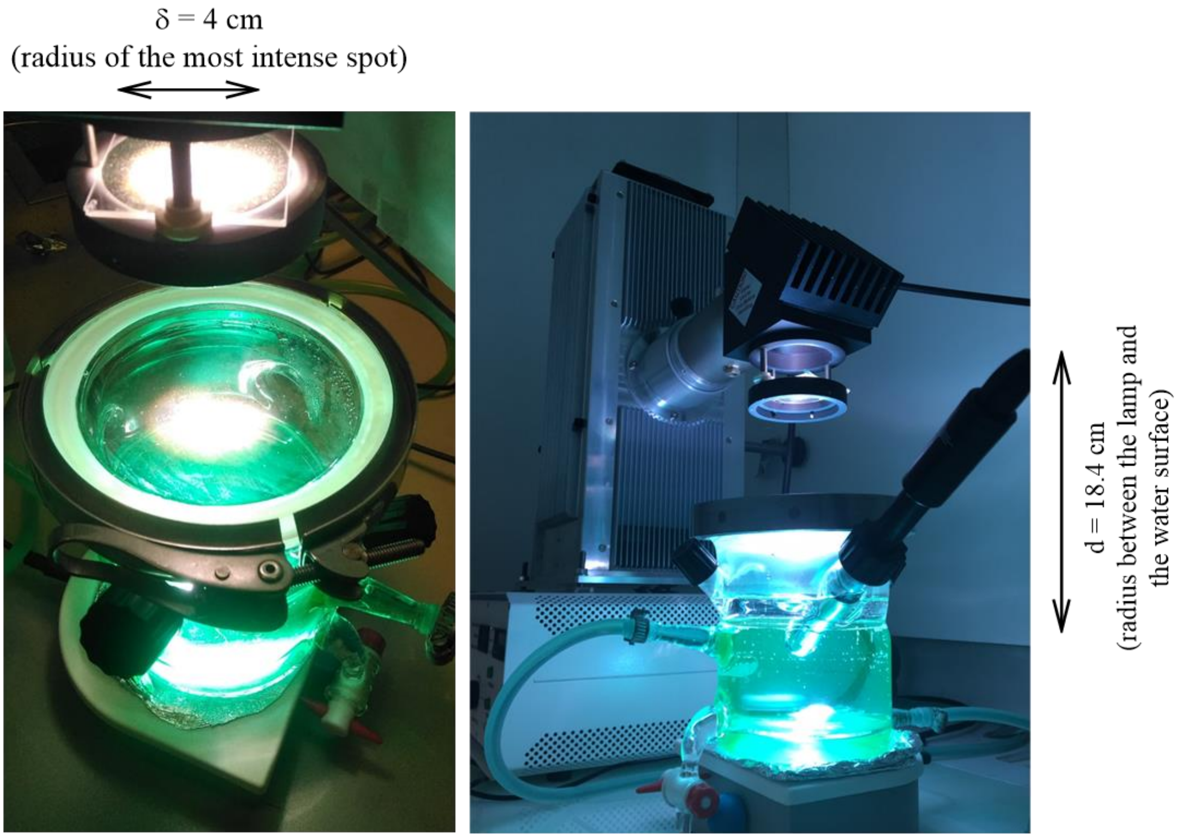

Figure S1: Experimental setup used for the photolysis experiments.

Section S1: Actinometry study

The lamp actinic flux that reaches the photoreactor was determined by performing an actinometry study with H_2O_2.

In a first step, the lamplight spectra were measured in the most intense spot of the lamplight (with a radius r = 2 cm, Fig. S1) at a distance of d = 18.2 cm using a spectrophotometer.

In a second step, the theoretical aqueous-phase photolysis rate constant of H_2O_2 ($J_{H_2O_2,calc.}$, in s^{-1}) was calculated using Eq. (S1):

$$J_{H_2O_2,calc.} = \int \sigma_{H_2O_2}(\lambda) \cdot \Phi_{H_2O_2}(\lambda) \cdot I(\lambda)_{meas.} \cdot d\lambda, \qquad \text{(S1)}$$

where $\sigma_{H_2O_2}(\lambda)$ is the aqueous-phase absorption cross-section values determined in this work (Table S2), $\Phi_{H_2O_2}(\lambda)$ is the recommended quantum yields values by Bianco et al., (2020), and $I(\lambda)_{meas.}$ is the lamp actinic flux measured in the first step. Using these data, one obtains an aqueous-phase H_2O_2 photolysis rate constant of 4.2×10^{-5} s^{-1}.

In a third step, the experimental photolysis rate constant of H_2O_2 ($J_{H_2O_2,exp.}$, in s^{-1}) was determined in the photoreactor during four photolysis experiments. The experimental protocol was the one used for $RONO_2$ photolysis experiments (described in Section 3.2), but experiments lasted 5 h instead of 7 h. The aqueous-phase concentration relative decay of H_2O_2 was monitored by offline UHPLC-UV analyses. During each photolysis experiment, H_2O_2 was consumed by its direct photolysis (RS1), but also by ·OH radicals (RS2) formed through H_2O_2 photolysis. H_2O_2 is also regenerated via $HO_2\cdot/O_2^{-}\cdot$ self-reactions (RS3 and RS4).

$$H_2O_2 + h\upsilon \rightarrow 2 \cdot OH \qquad \text{(RS1)}$$

$$H_2O_2 + \cdot OH \rightarrow HO_2 \cdot + H_2O \qquad \text{(RS2)}$$

$$2HO_2 \cdot \rightarrow H_2O_2 + O_2 \uparrow \qquad \text{(RS3)}$$

$$HO_2 \cdot + O_2^{-} \cdot \rightarrow HO_2^{-} + O_2 \uparrow \qquad \text{(RS4)}$$

Therefore, to account for all sources and sinks, the experimental H_2O_2 photolysis rate constant was determined using Eq. (S2):

$$ln\frac{[H_2O_2]_0}{[H_2O_2]_t} = 2 \cdot J_{H_2O_2,exp.} \cdot t, \qquad \text{(S2)}$$

where $[H_2O_2]_0/[H_2O_2]_t$ is the aqueous-phase concentration relative decay of H_2O_2 and t is the time (s). Equation (S2) is obtained by assuming steady-state of ·OH, $HO_2\cdot$, and $O_2^{-}\cdot$ radical concentrations. The determined aqueous-phase H_2O_2 photolysis rate constants of each photolysis experiment are compiled in Table S1 along with the initial conditions.

Table S1.1: actinometry study using H_2O_2: initial conditions and experimentally determined aqueous-phase photolysis rate constants.

Exp.	$[H_2O_2]_0$ (mM)	$J_{H_2O_2,exp.}$ ($\times 10^{-6}$ s^{-1})
1	20.5	7.2 ± 0.2
2	21.0	8.1 ± 0.3
3	22.4	7.6 ± 0.7
4	19.8	6.9 ± 0.8
Average		7.5 ± 0.5

Finally, the ratio of $J_{H_2O_2,calc.}$ to $J_{H_2O_2,exp.}$ (Eq. S3) represents the correction factor (cf).

$$cf = \frac{J_{H_2O_2,calc.}}{J_{H_2O_2,exp.}} \tag{S3}$$

Multiplying the correction factor to the measured, $I(\lambda)_{meas.}$, one obtains the lamp actinic flux that reaches the photoreactor (Eq. S4).

$$I(\lambda)_{reac.} = cf \cdot I(\lambda)_{meas.} \tag{S4}$$

The correction factor was determined to be 5.6.

Section S2: Determination of the experimental photolysis rate constants of $RONO_2$

As discussed in Section 3.2, the decay of $RONO_2$ in each photolysis experiment was not only due to its photolysis. Other processes such as evaporation (for isopropyl nitrate and isobutyl nitrate), hydrolysis (α-nitrooxyacetone), and/or ·OH oxidation (for all) contribute to their decay. Therefore, the decay of $RONO_2$ is given by Eq. (S5) during each photolysis experiment:

$$ln\frac{[RONO_2]_0}{[RONO_2]_t} = k' \cdot t = \left(J_{RONO_2} + k_{vap/hyd} + k_{OH}[\cdot OH]\right) \cdot t, \tag{S5}$$

where k' (s^{-1}) is the experimental total decay rate constant of $RONO_2$ which shows a pseudo-first order behavior at the beginning of the reaction when the ·OH-oxidation contributes to less than 10 % of the total decay (first two hours of reaction); k_{vap} and k_{hyd} (s^{-1}) are the evaporation and hydrolysis rate constants and were determined during control experiments (Table S4); k_{OH} is the aqueous-phase ·OH-oxidation rate constant and was taken from González-Sánchez et al., (2021); $[\cdot OH]$ is the concentration of ·OH radicals and was estimated assuming steady-state concentrations (using Eq. (S6)):

$$[\cdot OH] = \frac{J_{HNO_2}[HNO_2]+J_{NO_2^-}[NO_2^-]}{k_{OH,RONO_2}[RONO_2]+k_{OH,HNO_2}[HNO_2]+k_{OH,NO_2^-}[NO_2^-]}, \tag{S6}$$

where the photolysis rate constants of HNO_2 and NO_2^- (J_{HNO_2} and $J_{NO_2^-}$) were calculated using Eq. (S1), using absorption cross-sections from Fischer and Warneck, (1996); using quantum yields from Fischer and Warneck, (1996) for HNO_2 and from Herrmann, (2007) for NO_2^-; and using the corrected lamp actinic flux. The total concentration of HNO_2 and NO_2^- (written $[NO_2^-]_T$) was determined by High Pressure Ionic Chromatography measurements, and thus the concentration of each species was calculated using Eq. (S7) and Eq. (S8).

$$[HNO_2] = \frac{[NO_2^-]_T}{1+K_a/10^{-pH}} \tag{S7}$$

$$[NO_2^-] = [NO_2^-]_T - [HNO_2], \tag{S8}$$

where K_a is the acid dissociation constant of HNO_2, the pH was measured in all photolysis experiments (except during 1-nitrooxy-2-propanol photolysis experiments, for which average pH values were taken from the other experiments). Additionally, during α-nitrooxyacetone experiments, $[NO_2^-]_T$ was not measured and thus, average concentrations from other experiments were used instead. Table S2.1 lists the system of reactions that results in ·OH radical formation during $RONO_2$ photolysis with the corresponding reaction rate constants.

Table S2.1: Chemical reactions contributing to the formation and consumption of ·OH radicals during RONO2 photolysis.

Reaction	K_a, J or k_{OH}	Ref.	Nº
$RONO_2 + h\upsilon \rightarrow R'O + HNO_2$	J_{RONO2}		RS5
$HNO_2 + H_2O \rightarrow NO_2^- + H_3O^+$	$K_a = 7.1 \cdot 10^{-4}$ M	a	RS6
$NO_2^- + h\upsilon \rightarrow \cdot NO + \cdot O^-$	$J = 5.8 \cdot 10^{-5}\ s^{-1}$	a,b	RS7
$HNO_2 + h\upsilon \rightarrow \cdot NO + \cdot OH$	$J = 8.4 \cdot 10^{-4}\ s^{-1}$	a,b	RS8
$\cdot O^- + H_3O^+ \leftrightarrow \cdot OH + H_2O$	$K_a = 2.8 \cdot 10^{-12}$ M	c	RS9
$RONO_2 + \cdot OH \rightarrow products$	$k_{OH+RONO2}$	d	RS10
$NO_2^- + \cdot OH \rightarrow \cdot NO_2 + OH^-$	$k_{OH} = 1.0 \cdot 10^{10}\ M^{-1}\ s^{-1}$	a	RS11
$HNO_2 + \cdot OH \rightarrow \cdot NO_2 + H_2O$	$k_{OH} = 2.6 \cdot 10^{9}\ M^{-1}\ s^{-1}$	a	RS12

[a]Fischer and Warneck, (1996). [b]Herrmann, (2007) [c]Poskrebyshev et al., (2002) [d]González-Sánchez et al., (2021).

Table S2.2 lists the initial conditions for each photolysis experiment and the results: k' is the experimental decay rate constant at the beginning of the reaction (< 2 h) and the corresponding photolysis rate constant.

Table S2.2: RONO2 photolysis experiments: initial conditions and kinetic results.

Exp.	$RONO_2$	$[RONO_2]_0$	k' ($x10^{-5}$ s^{-1})	J_{RONO2} ($x10^{-6}$ s^{-1})
1	Isopropyl nitrate	0.93	1.7	5.9
2	Isopropyl nitrate	1.81	1.4	5.1
3	Isopropyl nitrate	1.71	1.0	3.9
4	Isobutyl nitrate	0.60	2.9	13.7
5	Isobutyl nitrate	0.59	2.5	10.3
6	Isobutyl nitrate	0.53	1.9	7.0
7	Isobutyl nitrate	0.55	2.6	10.7
8	Isobutyl nitrate	0.49	1.4	5.0
9	α-Nitrooxyacetone	1.18	0.59	3.1
10	1-Nitrooxy-2-propanol	0.72	0.49	3.8
11	1-Nitrooxy-2-propanol	0.38	0.52	4.3

Table S2.3 lists the initial conditions for each control experiment where k_{vap} or k_{hyd} were experimentally determined using Eq. (S9). The protocol of these experiments is the same as the one used during the photolysis experiments (Section 2.2), but they were performed under dark conditions.

$$ln\frac{[RONO_2]_0}{[RONO_2]_t} = k_{vap/hyd} \cdot t \tag{S9}$$

Table S2.3: RONO2 control experiments: initial conditions and kinetic results.

Exp.	$RONO_2$	$[RONO_2]_0$	k_{vap} ($x10^{-6}$ s^{-1})	k_{hyd} ($x10^{-6}$ s^{-1})
1	Isopropyl nitrate	0.84	9.7	–
2	Isopropyl nitrate	1.72	8.8	–
3	Isopropyl nitrate	1.66	5.6	–
4	Isopropyl nitrate	1.71	7.3	–
5	Isopropyl nitrate	1.82	6.5	–
6	Isobutyl nitrate	0.60	20.1	–
7	Isobutyl nitrate	0.52	8.1	–
8	Isobutyl nitrate	0.57	10.6	–
9	Isobutyl nitrate	0.57	20.8	–
10	α-Nitrooxyacetone	1.27	–	1.7
11	1-Nitrooxy-2-propanol	0.99	–	–
12	1-Nitrooxy-2-propanol	0.90	–	–
14	1-Nitrooxy-2-propanol	0.80	–	–

Table S1. List of the investigated compounds for absorption cross-section determinations in water or methanol at wavelengths ranging from 190 to 600 nm.

$RONO_2$	$[RONO_2]_0$ (mM)	Solvent
Isopropyl nitrate	0.5 – 2	H_2O
Isopropyl nitrate	1 – 10	CH_3OH
Isobutyl nitrate	1 – 10	CH_3OH
1-Pentyl nitrate	1 – 20	CH_3OH
Isopentyl nitrate	1 – 20	CH_3OH
2-Ethylhexyl nitrate	2 – 20	CH_3OH
α-Nitrooxyacetone	1 – 20	H_2O/CH_3OH (50/50, v/v)
1-Nitrooxy-2-propanol	1 – 10	H_2O
Isosorbide 5-mononitrate	1 – 20	H_2O
H_2O_2	1 – 25	H_2O

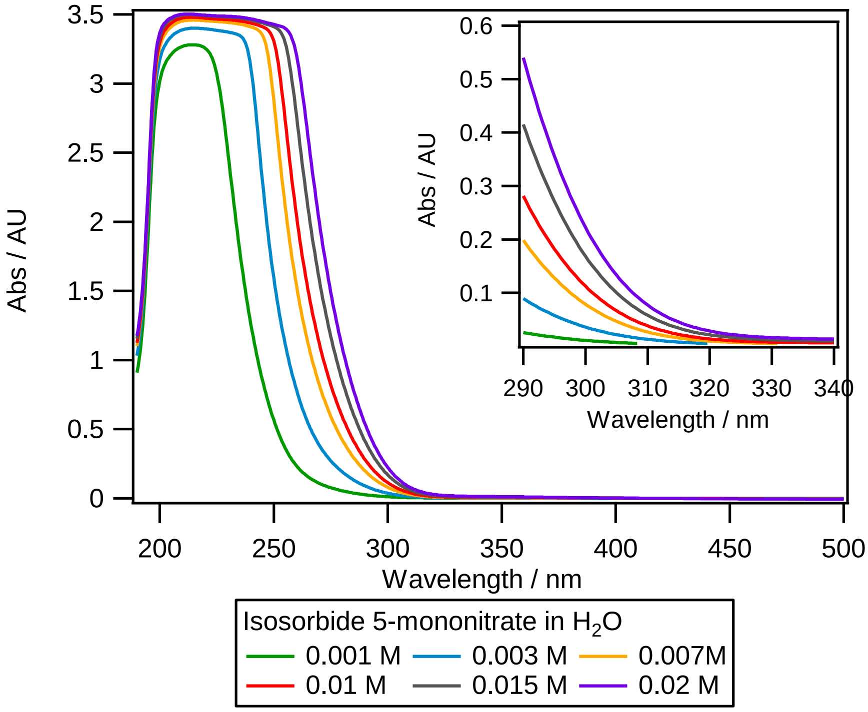

Figure S2. Absorption spectra of various aqueous solutions of isosorbide 5-mononitrate (from 0.001 to 0.02 M). The embedded graph represents the same data between 290 to 340 nm, the actinic region relevant for atmospheric photolysis

Section S3: Synthesis of α-nitrooxyacetone and 1-nitrooxy-2-propanol

α-Nitrooxyacetone 1.2 eq-mol of KI (98%, Sigma Aldrich) was added to a solution of chloroacetone (95%, Sigma Aldrich) in acetone. The solution was stirred in the dark at room temperature for 20 h. The mixture was filtered and concentrated under vacuum. The crude mixture was purified by silica gel column chromatography (pentane 10:1 ethyl acetate) leading to a deep brown oil. To an acetonitrile solution of iodoacetone, 1.5 eq-mol of $AgNO_3$ (99%, VWR Chemicals) was slowly added under dark conditions at 0 º C and stirred for 20 h at room temperature (under dark conditions). The precipitate was filtered and concentrated under vacuum. The crude mixture was purified by silica gel column chromatography (pentane 1:1 ethyl acetate) and lead to a yellow oil. ^{1}H-NMR (300 MHz, $CDCl_3$) δ: 2.24 (3H, s) 4.95 (2H, s). MS (EI): *m/z*: 43 (CH_3CO^+), 46 (NO_2^+), 57 ($CH_3COCH_2^+$), 76 ($CH_2ONO_2^+$).

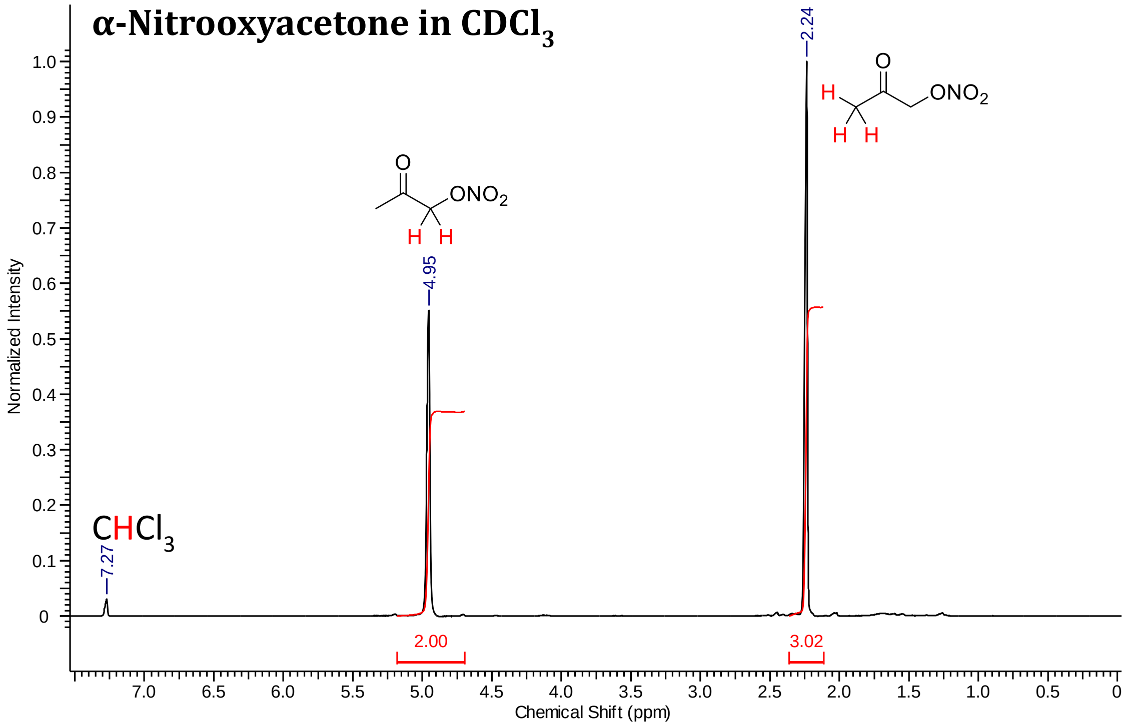

Figure S3.1. 1H-NMR spectra of α-nitrooxyacetone in CDCl3.

1-Nitrooxy-2-propanol. 0.4 eq-mol of $NaBH_4$ (98%, Sigma Aldrich) and a 0.2 eq-mol $NaHCO_3$ (99.7%, Sigma Aldrich) were added to a solution of α-nitrooxyacetone in ethanol at 0 ºC. The mixture was stirred at room temperature for 4 hours, concentrated under vacuum, and purified by silica gel column chromatography (pentane 3:1 ethyl acetate) to lead to a transparent oil. ^{1}H-NMR (300 MHz, D_2O) δ: 1.23 (3H, d, 6 Hz), 4.17 (1H, m), 4.42 (1H, m), 4.57 (1H, m). MS (EI): *m/z*: 45 ($CH_3CH(OH)^+$), 46 (NO_2^+), 59 ($CH_3CH(OH)CH_2^+$), 76 ($CH_2ONO_2^+$).

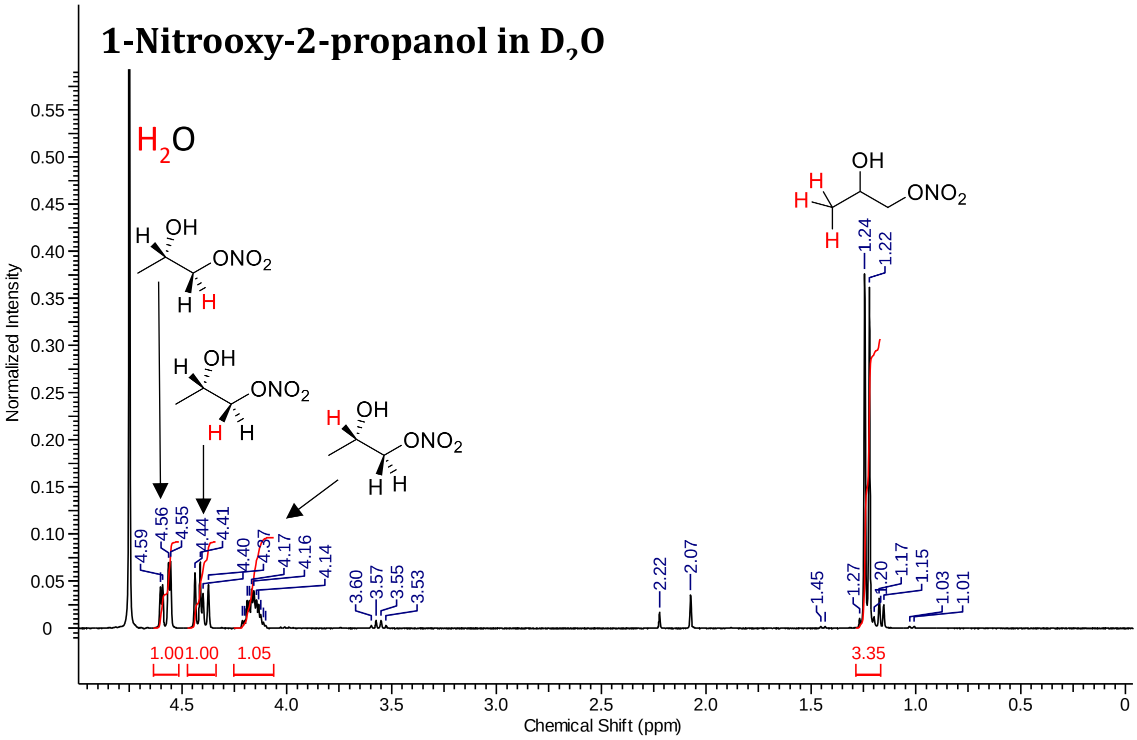

Figure S3.2. ^{1}H-NMR spectra of 1-nitrooxy-2-propanol in D_2O.

Section S4: Determination of the $RONO_2$ liquid-phase absorption cross-sections

The absorption cross-sections of each investigated compound were determined using Eq. (2):

$$Abs(\lambda) \cdot \ln 10 = \sigma(\lambda) \cdot L \cdot N \,, \tag{2}$$

where $Abs(\lambda)$ is the light absorbance of each $RONO_2$ at a determined wavelength, σ is the absorption cross-section of the molecule (in cm^2 $molec.^{-1}$) at a determined wavelength, N is the density of the molecule (molec. cm^{-3}), and L is the absorption path length (cm). By plotting $Abs \cdot ln\,10$ versus $L \cdot N$ one obtains a straight line with slope = $\sigma(\lambda)$ and the intercept at the origin.

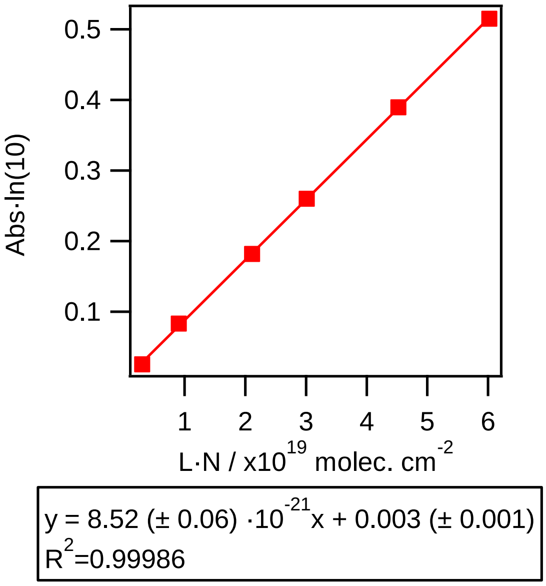

Figure S4.1. Determination of the aqueous-phase cross-sections of isosorbide 5-mononitrate at 300 nm between 0.001 to 0.02 M.

For each $RONO_2$, the absorption cross-sections between 290 to 340 nm were determined in the liquid phase (water or methanol). Absorbances were corrected by subtracting the signal measured between 360 to 500 nm (a region where no absorption occurs). An example of the determination of a cross-section value is given in Fig. S5. Although the methodology is simple, the presence of impurities with absorbing properties can entail significant deviations in the determination. Both α-nitrooxyacetone and 1-nitrooxy-2-propanol were synthesized and purified by a chromatographic column (Section S3). Despite this purification, small impurities were still suspected for both compounds, and thus the results obtained for these two compounds should be considered carefully.

Table S2. Experimentally determined liquid-phase absorption cross-sections of $RONO_2$.

$RONO_2$	Isopropyl nitrate	Isopropyl nitrate	Isobutyl nitrate	1-Pentyl nitrate	Isopentyl nitrate	2-Ethylhexyl nitrate	α-Nitrooxyacetone	1-Nitrooxy-2-propanol	Isosorbide 5-mononitrate
Solvent	**Water**	**Methanol**	**Methanol**	**Methanol**	**Methanol**	**Methanol**	**Me/Wa***	**Water**	**Water**
Wavelength / nm	**σ ($\cdot 10^{-20}$ cm^2 molec.$^{-1}$)**	**σ ($\cdot 10^{-20}$ cm^2 molec.$^{-1}$)**	**σ ($\cdot 10^{-20}$ cm^2 molec.$^{-1}$)**	**σ ($\cdot 10^{-20}$ cm^2 molec.$^{-1}$)**	**σ ($\cdot 10^{-20}$ cm^2 molec.$^{-1}$)**	**σ ($\cdot 10^{-20}$ cm^2 molec.$^{-1}$)**	**σ ($\cdot 10^{-20}$ cm^2 molec.$^{-1}$)**	**σ ($\cdot 10^{-20}$ cm^2 molec.$^{-1}$)**	**σ ($\cdot 10^{-20}$ cm^2 molec.$^{-1}$)**
290	1.95	1.98	2.19	2.29	2.34	12.17	3.03	2.07	1.98
292	1.69	1.77	1.91	1.99	2.05	10.97	2.67	1.76	1.77
294	1.44	1.57	1.65	1.71	1.79	9.90	2.33	1.49	1.57
296	1.22	1.38	1.42	1.46	1.55	8.97	2.03	1.25	1.38
298	1.03	1.20	1.21	1.24	1.34	8.17	1.77	1.03	1.20
300	0.86	1.04	1.02	1.04	1.14	7.47	1.53	0.85	1.04
302	0.70	0.90	0.85	0.86	0.97	6.87	1.32	0.70	0.90
304	0.58	0.77	0.71	0.70	0.81	6.36	1.14	0.57	0.77
306	0.46	0.66	0.58	0.57	0.68	5.94	0.99	0.46	0.66
308	0.37	0.55	0.47	0.46	0.57	5.60	0.85	0.37	0.55
310	0.29	0.46	0.38	0.37	0.47	5.33	0.74	0.29	0.46
312	0.23	0.39	0.31	0.29	0.39	5.12	0.65	0.24	0.39
314	0.17	0.32	0.25	0.22	0.33	4.98	0.57	0.19	0.32
316	0.13	0.27	0.20	0.16	0.27	4.87	0.51	0.16	0.27
318	0.10	0.22	0.16	0.12	0.23	4.80	0.46	0.13	0.22
320	0.08	0.19	0.13	0.09	0.20	4.76	0.41	0.11	0.19
322	0.06	0.15	0.10	0.06	0.17	4.74	0.38	0.09	0.15
324	0.04	0.13	0.09	0.04	0.15	4.74	0.35	0.08	0.13
326	0.03	0.11	0.07	0.03	0.13	4.73	0.33	0.07	0.11
328	0.03	0.09	0.06	0.02	0.12	4.72	0.31	0.07	0.09
330	0.02	0.07	0.06	0.01	0.11	4.72	0.29	0.06	0.07
332	0.02	0.06	0.05		0.10	4.72	0.28	0.06	0.06
334	0.02	0.05	0.05		0.10	4.72	0.26	0.06	0.05
336	0.01	0.04	0.04		0.09	4.69	0.25	0.06	0.04
338	0.01	0.04	0.04		0.09	4.64	0.24	0.05	0.04
340	0.01	0.03	0.04		0.08	4.58	0.23	0.05	0.03
345						4.39			
350						4.04			
355						3.59			
360						3.07			
365						2.51			
370						1.97			

375	1.52
380	1.13
385	0.84
390	0.62

[*] **Methanol/Water (50/50, v/v)**

Section S5: Deconvolution of the absorption cross-section spectra of α-nitrooxyacetone to remove the band observed above 320 nm which may be due to an impurity

To remove the band observed above 320 nm, the absorption cross-sections of α-nitrooxyacetone were deconvoluted into three gaussians by performing the fit of Eq. (S10) in our data.

$$f(x) = A_1 \mathrm{e}^{-\frac{(x-b_1)^2}{2\cdot {c_1}^2}} + A_2 \mathrm{e}^{-\frac{(x-b_2)^2}{2\cdot {c_2}^2}} + A_3 \mathrm{e}^{-\frac{(x-b_3)^2}{2\cdot {c_3}^2}} \tag{S10}$$

with initial guesses of $2 \cdot 10^{-18}$, 205, and 28 for A_1, b_1, and c_1, corresponding to the typical intense band of nitrooxy groups with a maximum at around 205 nm; of $6 \cdot 10^{-20}$, 270, and 20 for A_2, b_2, and c_2, corresponding to the carbonyl group band with a maximum at around 270 nm; and of $4.5 \cdot 10^{-20}$, 340, and 250 for A_3, b_3, and c_3, corresponding to the band observed above 320 nm and may potentially originate from an impurity.

Once the fit was calculated, the alternative absorption cross-sections of α-nitrooxyacetone in condensed phases was calculated by adding the first two gaussians. Using this absorption cross-section, a quantum yield average of 0.02 was calculated.

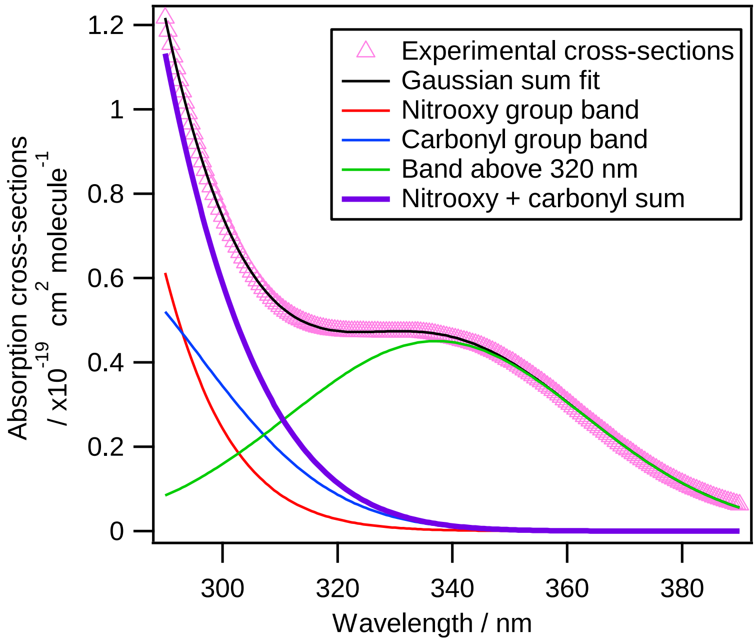

Figure S5.1. Deconvolution of the experimental absorption cross-sections of α-nitrooxyacetone into three absorption bands.

Section S6. Methodology for Section 4 calculations

Section S6.1. Calculation of $RONO_2$ partitioning and assignment of aqueous and gas phase J and k_{OH} for $RONO_2$ in Section 4.1

Partitioning. The partitioning of each molecule in the aqueous phase was calculated using Eq. (S10):

$$\varphi_{aq} = \frac{n_{aq}}{n_{aq}+n_{gas}} = \frac{1}{1+(1/LWC_v \cdot K_H \cdot R \cdot T)}, \tag{S10}$$

where φ_{aq} is the molar fraction of the compound in the aqueous phase, n_{aq} and n_{gas} are the number of moles of $RONO_2$ in the aqueous and the gas phase, respectively; K_H is the Henry's Law constant at standard conditions (in M atm^{-1}); R is the ideal gas constant (0.082 atm L mol^{-1} K^{-1}); T is the temperature (set at 298 K) and LWC_v is the liquid water content in volume units (m^3 of water/m^3 of air). Experimental K_H values were taken from (Sander, 2015) when available, or they were calculated using the GROHME method (Raventos-Duran et al., 2010).

·OH oxidation rate contants. Experimental values were used for $k_{OH,aq}$ and $k_{OH,gas}$ when available or they were calculated using the group contribution methods presented in González-Sánchez et al., (2021) and Jenkin et al., (2018), respectively.

Photolysis rate constants. J_{aq} and J_{gas} were calculated as described in Section 3 when experimental aqueous or gas-phase absorption cross-sections were available. When not available, average values were employed according to the molecule's chemical structure. For all investigated $RONO_2$, a unique J_{aq} value of $3.9 \cdot 10^{-7}$ s^{-1} was considered. This value is the average of eight $RONO_2$ molecules bearing a carbonyl or a hydroxy group: α-nitrooxyacetone, 1-nitrooxy-2-propanol, isosorbide 5-mononitrate, and compounds A, B, C, D, and F in Table 2. This value is likely a good approximation since all the $RONO_2$ photolysis rate constants determined in this work fall in the same order of magnitude and do not present significant deviations (Table 2). For $RONO_2$ with undetermined gas-phase absorption cross-sections, three J_{gas} values were used depending on their chemical structure. A high value ($6.6 \cdot 10^{-5}$ s^{-1}) was used for carbonyl nitrates since these compounds present an enhancement in their photolysis rates compared to alkyl nitrates. This value was averaged from all carbonyl nitrates J_{gas} values available in the literature (see Table S5). For the C_5 dihydroxy dinitrate compound, a value of $4.4 \cdot 10^{-6}$ s^{-1} was chosen, averaged from dinitrates photolysis rate constants. For other $RONO_2$, a value of $7.6 \cdot 10^{-7}$ s^{-1} was chosen, averaged from photolysis rate constants of alkyl nitrates with more than 2 carbon atoms.

Section S6.2. Assignment of J and k_{OH} for $RONO_2$ in Section 4.2

The aqueous phase and gas phase photolysis and ·OH-oxidation rate constants were assumed or estimated as described in Section S6.1. Nevertheless, eight of the investigated molecules (all the allylic $RONO_2$ and *tert* 1, 2, 5, and 6) bear an unsaturation in their chemical structure, and thus their aqueous-phase ·OH-oxidation rate constant cannot be calculated with the Structure-Activity Relationship (SAR). For these compounds, a rate constant of 10^{10} M^{-1} s^{-1} was assumed. This assumption is based on the high reactivities (close to the diffusion limit) of unsaturated molecules due the ·OH addition on the double bond (Herrmann et al., 2015). Besides, it should be noted that no experimental photolysis rate constants were reported for allylic $RONO_2$ in any phase. Hence, the assumed photolysis rate constants have to been taken with caution.

Section S6.3. Assignment of dry and wet k_{dep} for $RONO_2$ in Section 4.3

Dry deposition rate constants were calculated considering a boundary height layer of 1000 m. The average daytime deposition velocities were assigned based on the chemical structure of the $RONO_2$. For alkyl nitrates, a value of 0.15 cm s^{-1} (averaged from values determined by Abeleira et al., (2018) for $RONO_2$ bearing three to five carbon atoms). For terpene nitrates, a value of 0.8 cm s^{-1} was assumed (corresponding to the value determined by Nguyen et al., (2015) for two terpene nitrates). For the rest of $RONO_2$, i.e., polyfunctional $RONO_2$ bearing less than 10 carbon atoms, a value of 1.5 cm s^{-1} was assumed (averaged from values determined by Nguyen et al., (2015) for four isoprene nitrates).

Wet deposition lifetimes were estimated from Brimblecombe and Dawson, (1984) using Eq. (S11):

$$k_{wd} = \frac{\mathrm{R}_r E e^{-z/H_x}}{H_x((K_H R T^{-1}) + L_{WC})}, \tag{S11}$$

where k_{wd} is the wet deposition rate constant (in s^{-1}), R_r is the assumed annual rainfall rate (3.17×10^{-8} m s^{-1} or 1 m yr^{-1}), E is the enhancement due to droplet evaporation (set at 1.33), z is the characteristic height for clouds (set at 3500 m), H_x is the scale height for the molecules (set at 2200 m), and L_{WC} is the liquid water content of the cloud (3.5×10^{-7} m^3 of water/m^3 of air).

Since the rainfall rate is assumend yearly, wet deposition rate constants are considered equal in both cloud/fog and wet aerosol scenarios.

Table S3. Atmospherically relevant non-hydrolyzable $RONO_2$ Henry's Law constants, aqueous-phase and gas-phase ·OH-oxidation rate constants, aqueous-phase and gas-phase photolysis rate constants, molar fractions, and multiphase lifetimes at cloud/fog (LWC = 0.35 g m^{-3}) and wet aerosol (LWC = 3 ·10^{-5} g m^{-3}) conditions.

<table>
<tr><th colspan="11">Small $RONO_2$</th></tr>
<tr><th rowspan="2">$RONO_2$ structure</th><th rowspan="2">Name</th><th rowspan="2">K_H (M atm^{-1})</th><th rowspan="2">$k_{OH, aq}$ (M^{-1} s^{-1})</th><th rowspan="2">$k_{OH, gas}$ (cm^3 molec.$^{-1}$ s^{-1})</th><th rowspan="2">J_{aq} (s^{-1})</th><th rowspan="2">J_{gas} (s^{-1})</th><th colspan="2">Cloud/fog conditions (LWC = 0.35 g m^{-3})</th><th colspan="2">Wet aerosol conditions (LWC = 3 × 10^{-5} g m^{-3})</th></tr>
<tr><th>φ_{aq} (%)</th><th>τ_{mult} (h)</th><th>φ_{aq} (%)</th><th>τ_{mult} (h)</th></tr>
<tr><td>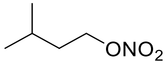</td><td>Isopentyl nitrate</td><td>0.45</td><td>2.22×10^{9}</td><td>2.37×10^{-12}</td><td>4.90×10^{-7}</td><td>7.57×10^{-7}</td><td>0.0</td><td>50</td><td>0.0</td><td>50</td></tr>
<tr><td>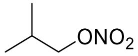</td><td>Isobutyl nitrate</td><td>0.54</td><td>1.74×10^{9}</td><td>1.43×10^{-12}</td><td>5.90×10^{-7}</td><td>5.25×10^{-7}</td><td>0.0</td><td>69</td><td>0.0</td><td>69</td></tr>
<tr><td>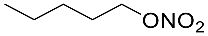</td><td>1-Pentyl nitrate</td><td>0.60</td><td>3.11×10^{9}</td><td>3.13×10^{-12}</td><td>3.04×10^{-7}</td><td>8.89×10^{-7}</td><td>0.0</td><td>41</td><td>0.0</td><td>41</td></tr>
<tr><td>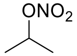</td><td>Isopropyl nitrate</td><td>0.62</td><td>2.84×10^{8}</td><td>3.48×10^{-13}</td><td>3.21×10^{-7}</td><td>8.66×10^{-7}</td><td>0.0</td><td>97</td><td>0.0</td><td>97</td></tr>
<tr><td>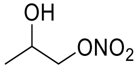</td><td>1-Nitrooxy-2-propanol</td><td>1.10×10^{4}</td><td>8.72×10^{8}</td><td>5.10×10^{-12}</td><td>4.20×10^{-7}</td><td>4.88×10^{-9}</td><td>5.4</td><td>12</td><td>0.0</td><td>12</td></tr>
<tr><td>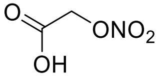</td><td>Nitrooxyacetic acid</td><td>1.62×10^{5}</td><td>2.65×10^{7}</td><td>5.99×10^{-12}</td><td>3.95×10^{-7}</td><td>7.57×10^{-7}</td><td>58.1</td><td>12</td><td>0.0</td><td>12</td></tr>
<tr><th colspan="11">Isoprene nitrates</th></tr>
<tr><th rowspan="2">$RONO_2$ structure</th><th rowspan="2">Name</th><th rowspan="2">K_H (M atm^{-1})</th><th rowspan="2">$k_{OH, aq}$ (M^{-1} s^{-1})</th><th rowspan="2">$k_{OH, gas}$ (cm^3 molec.$^{-1}$ s^{-1})</th><th rowspan="2">J_{aq} (s^{-1})</th><th rowspan="2">J_{gas} (s^{-1})</th><th colspan="2">Cloud/fog conditions (LWC = 0.35 g m^{-3})</th><th colspan="2">Wet aerosol conditions (LWC = 3 × 10^{-5} g m^{-3})</th></tr>
<tr><th>φ_{aq} (%)</th><th>τ_{mult} (h)</th><th>φ_{aq} (%)</th><th>τ_{mult} (h)</th></tr>
<tr><td>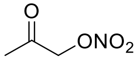</td><td>α-Nitrooxyacetone</td><td>1.01×10^{3}</td><td>7.91×10^{7}</td><td>4.33×10^{-13}</td><td>5.51×10^{-8}</td><td>1.29×10^{-5}</td><td>0.9</td><td>9</td><td>0.0</td><td>9</td></tr>
</table>

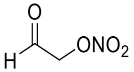	Ethanal nitrate	6.17×10^{3}	5.53×10^{8}	7.44×10^{-12}	3.95×10^{-7}	6.15×10^{-5}	5.0	3	0.0	3
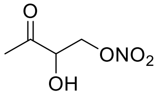	Methyl vinyl ketone nitrate' (MVKN')	9.55×10^{4}	2.99×10^{8}	2.47×10^{-12}	3.95×10^{-7}	1.45×10^{-5}	45.0	9	0.0	7
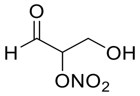	Methyl vinyl ketone nitrate (MVKN)	1.86×10^{5}	5.38×10^{8}	3.89×10^{-12}	3.95×10^{-7}	2.55×10^{-5}	61.4	7	0.0	5
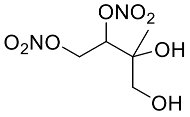	C_5 dihydroxy dinitrate	8.71×10^{7}	1.12×10^{9}	8.36×10^{-12}	3.95×10^{-7}	4.42×10^{-6}	99.9	7	6.0	7
Terpene nitrates										
$RONO_2$ structure	**Name**	**K_H (M atm^{-1})**	**$k_{OH, aq}$ (M^{-1} s^{-1})**	**$k_{OH, gas}$ (cm^3 molec.$^{-1}$ s^{-1})**	**J_{aq} (s^{-1})**	**J_{gas} (s^{-1})**	**Cloud/fog conditions (LWC = 0.35 g m^{-3})**		**Wet aerosol conditions (LWC = 3 × 10^{-5} g m^{-3})**	
							φ_{aq} (%)	**τ_{mult} (h)**	**φ_{aq} (%)**	**τ_{mult} (h)**
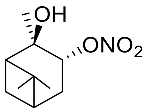	α-pinen 1	8.32×10^{3}	2.83×10^{9}	6.56×10^{-12}	3.95×10^{-7}	7.57×10^{-7}	6.6	14	0.0	15
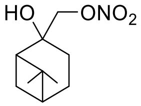	β-pinen 1	8.71×10^{3}	3.91×10^{9}	9.23×10^{-12}	3.95×10^{-7}	7.57×10^{-7}	6.9	11	0.0	12
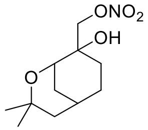	β-pinen 2	5.62×10^{5}	2.99×10^{9}	2.04×10^{-11}	3.95×10^{-7}	7.57×10^{-7}	82.8	6	0.0	6

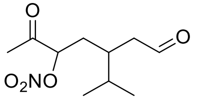	γ-terpinen 1	1.02×10^{6}	5.46×10^{9}	3.50×10^{-11}	3.95×10^{-7}	6.57×10^{-5}	89.8	4	0.1	2
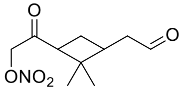	β-pinen 3	3.72×10^{6}	4.22×10^{9}	2.87×10^{-11}	3.95×10^{-7}	6.57×10^{-5}	97.0	4	0.3	2
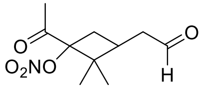	α-pinen 2	4.57×10^{6}	3.56×10^{9}	2.66×10^{-11}	3.95×10^{-7}	6.57×10^{-5}	97.5	5	0.3	2
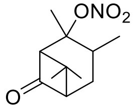	α-pinen 3	2.34×10^{7}	1.78×10^{9}	6.21×10^{-12}	3.95×10^{-7}	7.57×10^{-7}	99.5	7	1.7	10
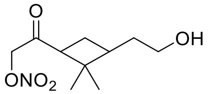	β-pinen 4	3.98×10^{7}	4.54×10^{9}	1.12×10^{-11}	3.95×10^{-7}	6.57×10^{-5}	99.7	4	2.8	3
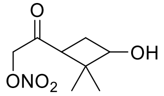	β-pinen 5	5.01×10^{7}	2.48×10^{9}	8.63×10^{-12}	3.95×10^{-7}	6.57×10^{-5}	99.8	6	3.5	3
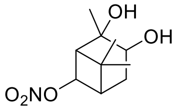	α-pinen 4	2.24×10^{8}	2.50×10^{9}	2.23×10^{-11}	3.95×10^{-7}	7.57×10^{-7}	100.0	6	14.1	6
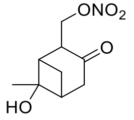	β-pinen 6	2.95×10^{8}	2.64×10^{9}	1.34×10^{-11}	3.95×10^{-7}	6.57×10^{-5}	100.0	6	17.8	3
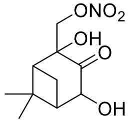	β-pinen 7	1.32×10^{9}	2.47×10^{9}	6.56×10^{-12}	3.95×10^{-7}	6.57×10^{-5}	100.0	6	49.2	4

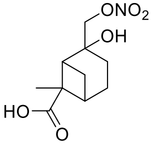	β-pinen 8	3.39×10^{9}	3.54×10^{9}	1.39×10^{-11}	3.95×10^{-7}	7.57×10^{-7}	100.0	5	71.3	6
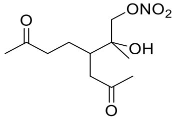	limonen 1	1.12×10^{10}	4.00×10^{9}	4.58×10^{-11}	3.95×10^{-7}	7.57×10^{-7}	100.0	5	89.1	4
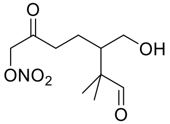	β-pinen 9	3.39×10^{10}	6.20×10^{9}	5.49×10^{-11}	3.95×10^{-7}	6.57×10^{-5}	100.0	3	96.1	3
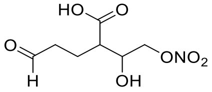	myrcen 1	4.37×10^{10}	3.49×10^{9}	3.70×10^{-11}	3.95×10^{-7}	7.57×10^{-7}	100.0	5	97.0	5
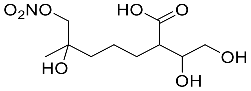	myrcen 2	4.90×10^{10}	5.41×10^{9}	2.55×10^{-11}	3.95×10^{-7}	7.57×10^{-7}	100.0	4	97.3	4
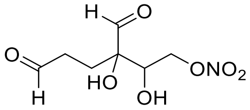	myrcen 3	7.41×10^{10}	2.85×10^{9}	4.86×10^{-11}	3.95×10^{-7}	7.57×10^{-7}	100.0	6	98.2	6
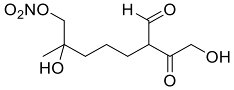	myrcen 4	2.34×10^{11}	4.79×10^{9}	4.05×10^{-11}	3.95×10^{-7}	7.57×10^{-7}	100.0	4	99.4	4
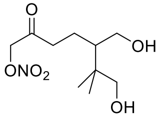	β-pinen 10	3.24×10^{11}	6.43×10^{9}	2.01×10^{-11}	3.95×10^{-7}	6.57×10^{-5}	100.0	3	99.6	3

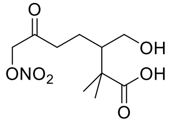	β-pinen 11	4.17×10^{12}	4.55×10^{9}	2.45×10^{-11}	3.95×10^{-7}	6.57×10^{-5}	100.0	4	100.0	4

Table S4. Atmospherically relevant hydrolyzable $RONO_2$ Henry's Law constants, aqueous-phase and gas-phase ·OH-oxidation rate constants, aqueous-phase and gas-phase photolysis rate constants, and molar fractions and multiphase lifetimes at cloud/fog (LWC = 0.35 g m^{-3}) and wet aerosol (LWC = 3 ·10^{-5} g m^{-3}) conditions.

Tertiary $RONO_2$											
Chemical structure	**Name**	**K_H (M atm^{-1})**	**k_{hyd} (s^{-1})**	**$k_{OH, aq}$ (M^{-1} s^{-1})**	**$k_{OH, gas}$ (cm^3 molec.$^{-1}$ s^{-1})**	**J_{aq} (s $^{-1}$)**	**J_{gas} (s^{-1})**	**Cloud/fog conditions**		**Wet aerosol conditions**	
								φ_{aq} (%)	**τ_{mult} (h)**	**φ_{aq} (%)**	**τ_{mult} (h)**
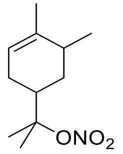	tert 1[a]	1.3	3.2×10^{-5}	1.00×10^{10}	9.90×10^{-11}	3.95×10^{-7}	7.57×10^{-7}	0.0	2	0.0	2
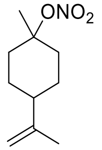	tert 2[b]	1.7	9.2×10^{-4}	1.00×10^{10}	6.58×10^{-11}	3.95×10^{-7}	7.57×10^{-7}	0.0	3	0.0	3
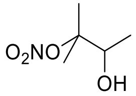	tert 3[c]	2.0×10^{3}	9.3×10^{-3}	7.07×10^{8}	2.40×10^{-12}	3.95×10^{-7}	7.57×10^{-7}	1.7	2	0.0	14
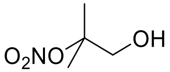	tert 4[c]	2.6×10^{3}	9.3×10^{-3}	5.54×10^{8}	1.17×10^{-12}	3.95×10^{-7}	7.57×10^{-7}	2.2	1	0.0	16
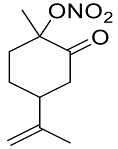	tert 5[b]	4.6×10^{3}	3.7×10^{-5}	1.00×10^{10}	6.87×10^{-11}	3.95×10^{-7}	6.57×10^{-5}	3.8	2	0.0	2

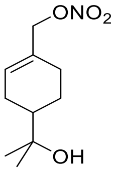	tert 6[b]	5.6×10^{4}	1.1×10^{-4}	1.00×10^{10}	1.72×10^{-10}	3.95×10^{-7}	7.57×10^{-7}	32.5	1	0.0	1
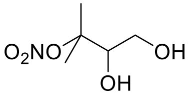	tert 7[d]	3.6×10^{6}	2.3×10^{-3}	1.11×10^{9}	1.28×10^{-11}	3.95×10^{-7}	7.57×10^{-7}	96.9	0.1	0.3	5
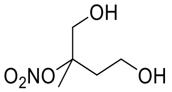	tert 8[d]	5.0×10^{6}	4.6×10^{-3}	2.27×10^{9}	5.71×10^{-12}	3.95×10^{-7}	7.57×10^{-7}	97.7	0.1	0.4	5
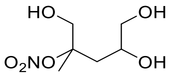	tert 9[d]	2.1×10^{10}	4.1×10^{-4}	1.39×10^{9}	2.91×10^{-11}	3.95×10^{-7}	7.57×10^{-7}	100.0	0.6	94.0	0.6
Allylic $RONO_2$											
Chemical structure	**Name**	**K_H (M atm^{-1})**	**k_{hyd} (s^{-1})**	**$k_{OH, aq}$ (M^{-1} s^{-1})**	**$k_{OH, gas}$ (cm^3 molec.$^{-1}$ s^{-1})**	**J_{aq} (s^{-1})**	**J_{gas} (s^{-1})**	**Cloud/fog conditions**		**Wet aerosol conditions**	
								φ_{aq} (%)	**τ_{mult} (h)**	**φ_{aq} (%)**	**τ_{mult} (h)**
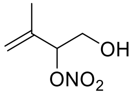	ally 1[e]	8.3×10^{3}	1.6×10^{-5}	1.00×10^{10}	3.90×10^{-11}	3.95×10^{-7}	7.57×10^{-7}	6.6	4	0.0	4

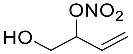	ally 2[e]	1.1×10^{4}	9.9×10^{-6}	1.00×10^{10}	1.92×10^{-11}	3.95×10^{-7}	7.57×10^{-7}	8.6	5	0.0	6
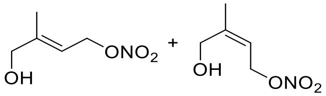	ally 3[e]	4.8×10^{4}	6.8×10^{-3}	1.00×10^{10}	1.10×10^{-10}	3.95×10^{-7}	7.57×10^{-7}	29.0	0.1	0.0	2
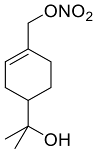	ally 4[b]	6.2×10^{4}	1.2×10^{-3}	1.00×10^{10}	6.18×10^{-11}	3.95×10^{-7}	7.57×10^{-7}	34.5	0.5	0.0	3

k_{hyd} taken from [a]Rindelaub et al., (2015)**;** [b]Wang et al., (2021)**;** [c]Hu et al., (2011)**;** [d]Darer et al., (2011) **and** [e]Jacobs et al., (2014)**.**

Table S5. Gas-phase photolysis rate constants and lifetimes for alkyl nitrates, dinitrates and carbonyl nitrates reported from the literature.

Alkyl nitrates

$RONO_2$	Name	Global J ($\times 10^{-6}$ s^{-1})	Global $\tau_{h\upsilon}$ (days)	Ref.
CH_3ONO_2	Methyl nitrate	0.12	93	a
		0.35	33	b
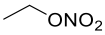	Ethyl nitrate	0.18	66	a
		0.57	20	b
		0.59	20	c
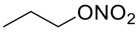	1-Propyl nitrate	0.25	47	a
		0.75	15	c
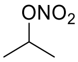	Isopropyl nitrate	0.68	17	a
		1.00	12	b
		0.92	13	c
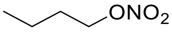	1-Butyl nitrate	0.76	15	c
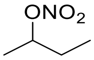	2-Butyl nitrate	0.52	22	a
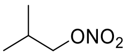	Isobutyl nitrate	0.22	53	a
		0.83	14	c
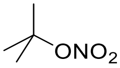	*tert*-butyl nitrate	2.64	4	a
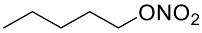	1-Pentyl nitrate	0.89	13	c
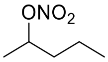	2-Pentyl nitrate	0.33	36	a
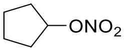	Cyclopentyl nitrate	0.06	183	a

Dinitrates

$RONO_2$	Summer J ($\cdot 10^{-6}$ s^{-1})	Global J $\cdot$ (10^{-6} s^{-1})	Global $\tau_{h\upsilon}$ (days)	Ref.
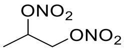	1,2-propyl dinitrate	4.5	2.6	d
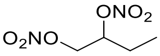	1,2-butyl dinitrate	6.3	1.8	d
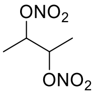	2,3-butyl dinitrate	4.5	2.6	d
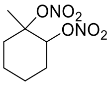	*trans*-1-methylcyclohexyl-1,2-dinitrate	7.4	1.6	e
	*cis*-1,4-Dinitrooxy-2-butene	2.6	4.5	d
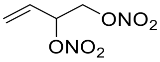	3,4-Dinitrooxy-2-butene	1.2	10.0	d

Hydroxy nitrates				
$RONO_2$	**Summer J ($\cdot 10^{-6}$ s^{-1})**	**Global J · (10^{-6} s^{-1})**	**Global $\tau_{h\upsilon}$ (days)**	**Ref.**
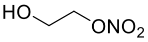	1-Nitrooxyethanol	0.005	2400	a
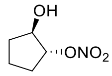	*trans*-2-Hydroxy-cyclopentyl-1-nitrate	0	∞	e
Carbonyl nitrates				
$RONO_2$	**Summer J ($\cdot 10^{-6}$ s^{-1})**	**Global J · (10^{-6} s^{-1})**	**Global $\tau_{h\upsilon}$ (hours)**	**Ref.**
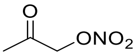	α-Nitrooxyacetone	11 15	24 19	a d
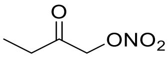	1-Nitrooxy-2-butanone	7.6	37	d
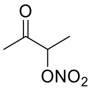	3-Nitrooxy-2-butanone	22	13	d
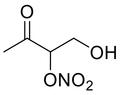	Methylvinylketone nitrate	25	11	f
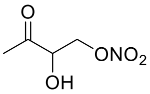	Methylvinylketone nitrate’	15	19	f
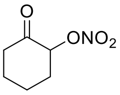	2-Oxo-cyclohexyl-1-nitrate	1	199	e
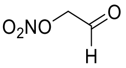	Ethanal nitrate	61	5	f
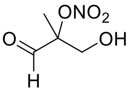	Methacrolein nitrate	149	2	f
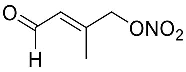	4,1-Nitrooxy enal	295	1	f

[a] Roberts and Fajer, (1989). [b] Talukdar et al., (1997). [c] Clemitshaw et al., (1997). [d] Barnes et al., (1993). [e] Wängberg et al., (1996) [f] Müller et al., (2014).

References

Abeleira, A., Sive, B., Swarthout, R. F., Fischer, E. V., Zhou, Y., and Farmer, D. K.: Seasonality, sources and sinks of C1-C5 alkyl nitrates in the Colorado Front Range, Elementa, 6, https://doi.org/10.1525/ELEMENTA.299/112816, 2018.

Barnes, I., Becker, K. H., and Zhu, T.: Near UV absorption spectra and photolysis products of difunctional organic nitrates: Possible importance as NOx reservoirs, J Atmos Chem, 17, 353–373, https://doi.org/10.1007/BF00696854, 1993.

Bianco, A., Passananti, M., Brigante, M., and Mailhot, G.: Photochemistry of the cloud aqueous phase: A review, https://doi.org/10.3390/molecules25020423, 20 January 2020.

Brimblecombe, P. and Dawson, G. A.: Wet removal of highly soluble gases, Journal of Atmospheric Chemistry 1984 2:1, 2, 95–107, https://doi.org/10.1007/BF00127265, 1984.

Clemitshaw, K. C., Williams, J., Rattigan, O. v., Shallcross, D. E., Law, K. S., and Anthony Cox, R.: Gas-phase ultraviolet absorption cross-sections and atmospheric lifetimes of several C2-C5 alkyl nitrates, J Photochem Photobiol A Chem, 102, 117–126, https://doi.org/10.1016/S1010-6030(96)04458-9, 1997.

Darer, A. I., Cole-Filipiak, N. C., O'Connor, A. E., and Elrod, M. J.: Formation and stability of atmospherically relevant isoprene-derived organosulfates and organonitrates, Environ Sci Technol, 45, 1895–1902, https://doi.org/10.1021/es103797z, 2011.

Fischer, M. and Warneck, P.: Photodecomposition of nitrite and undissociated nitrous acid in aqueous solution, Journal of Physical Chemistry, 100, 18749–18756, https://doi.org/10.1021/jp961692+, 1996.

González-Sánchez, J. M., Brun, N., Wu, J., Morin, J., Temime-Rousell, B., Ravier, S., Mouchel-Vallon, C., Clément, J.-L., and Monod, A.: On the importance of atmospheric loss of organic nitrates by aqueous-phase ·OH-oxidation, Atmos Chem Phys, 21, 4915–4937, https://doi.org/10.5194/acp-2020-684, 2021.

Herrmann, H.: On the photolysis of simple anions and neutral molecules as sources of O-/OH, SOx- and Cl in aqueous solution, https://doi.org/10.1039/b618565g, 23 July 2007.

Herrmann, H., Schaefer, T., Tilgner, A., Styler, S. A., Weller, C., Teich, M., and Otto, T.: Tropospheric Aqueous-Phase Chemistry: Kinetics, Mechanisms, and Its Coupling to a Changing Gas Phase, Chem Rev, 115, 4259–4334, https://doi.org/10.1021/cr500447k, 2015.

Hu, K. S., Darer, A. I., and Elrod, M. J.: Thermodynamics and kinetics of the hydrolysis of atmospherically relevant organonitrates and organosulfates, Atmos Chem Phys, 11, 8307–8320, https://doi.org/10.5194/acp-11-8307-2011, 2011.

Jacobs, M. I., Burke, W. J., and Elrod, M. J.: Kinetics of the reactions of isoprene-derived hydroxynitrates: Gas phase epoxide formation and solution phase hydrolysis, Atmos Chem Phys, 14, 8933–8946, https://doi.org/10.5194/acp-14-8933-2014, 2014.

Jenkin, M. E., Valorso, R., Aumont, B., Rickard, A. R., and Wallington, T. J.: Estimation of rate coefficients and branching ratios for gas-phase reactions of OH with aliphatic organic compounds for use in automated mechanism construction, Atmos Chem Phys, 18, 9297–9328, https://doi.org/10.5194/acp-18-9297-2018, 2018.

Müller, J. F., Peeters, J., and Stavrakou, T.: Fast photolysis of carbonyl nitrates from isoprene, Atmos Chem Phys, 14, 2497–2508, https://doi.org/10.5194/acp-14-2497-2014, 2014.

Nguyen, T. B., Crounse, J. D., Teng, A. P., Clair, J. M. S., Paulot, F., Wolfe, G. M., and Wennberg, P. O.: Rapid deposition of oxidized biogenic compounds to a temperate forest, Proc Natl Acad Sci U S A, 112, E392–E401, https://doi.org/10.1073/pnas.1418702112, 2015.

Poskrebyshev, G. A., Neta, P., and Huie, R. E.: Temperature Dependence of the Acid Dissociation Constant of the Hydroxyl Radical, J Phys Chem A, 106, 11488–11491, https://doi.org/10.1021/jp020239x, 2002.

Raventos-Duran, T., Camredon, M., Valorso, R., Mouchel-Vallon, C., and Aumont, B.: Structure-activity relationships to estimate the effective Henry's law constants of organics of atmospheric interest, Atmos Chem Phys, 10, 7643–7654, https://doi.org/10.5194/acp-10-7643-2010, 2010.

Rindelaub, J. D., McAvey, K. M., and Shepson, P. B.: The photochemical production of organic nitrates from α-pinene and loss via acid-dependent particle phase hydrolysis, Atmos Environ, 100, 193–201, https://doi.org/10.1016/j.atmosenv.2014.11.010, 2015.

Roberts, J. M. and Fajer, R. W.: UV Absorption Cross Sections of Organic Nitrates of Potential Atmospheric Importance and Estimation of Atmospheric Lifetimes, Environ Sci Technol, 23, 945–951, https://doi.org/10.1021/es00066a003, 1989.

Sander, R.: Compilation of Henry's law constants (version 4.0) for water as solvent, Atmos Chem Phys, 15, 4399–4981, https://doi.org/10.5194/acp-15-4399-2015, 2015.

Talukdar, R. K., Burkholder, J. B., Hunter, M., Gilles, M. K., Roberts, J. M., and Ravishankara, A. R.: Atmospheric fate of several alkyl nitrates: Part 2. UV absorption cross-sections and photodissociation quantum yields, Journal of the Chemical Society - Faraday Transactions, 93, 2797–2805, https://doi.org/10.1039/a701781b, 1997.

Wang, Y., Piletic, I. R., Takeuchi, M., Xu, T., France, S., and Ng, N. L.: Synthesis and Hydrolysis of Atmospherically Relevant Monoterpene-Derived Organic Nitrates, Environ Sci Technol, 55, 14595–14606, https://doi.org/10.1021/acs.est.1c05310, 2021.

Wängberg, I., Barnes, I., and Becker, K. H.: Atmospheric chemistry of bifunctional cycloalkyl nitrates, Chem Phys Lett, 261, 138–144, https://doi.org/10.1016/0009-2614(96)00857-3, 1996.